ELSEVIER

Earth and Planetary Science Letters 148 (1997) 157–170

EPSL

Forces controlling the present-day state of stress in the Andes

P.Th. Meijer [a,*], R. Govers [b,1], M.J.R. Wortel [a]

[a] *Geodynamics Research Institute, Faculty of Earth Sciences, Utrecht University, P.O. Box 80.021, 3508 TA Utrecht, The Netherlands*
[b] *Department of Geosciences, Penn State University, 439 Deike Building, University Park, PA 16802, USA*

Received 18 December 1996; revised 30 January 1997; accepted 6 February 1997

Abstract

The present-day state of stress in the Andes is expected to be controlled primarily by two different types of forces: (1) the resistive force exerted on the western overriding margin of the South American plate, and (2) forces that arise from the thickened crust of the Andes (i.e., the effect of topography and its compensating crustal root). We have studied these forces on the basis of a model for the dynamics of the entire South American plate in which the Andes are embedded. In this model a given set of forces is constrained by the criterion that the net torque on the plate should vanish. A thin elastic shell representation is used to calculate the intra-plate stress field associated with the various force distributions. We define a reference model for the present study that incorporates a uniform magnitude for the resistance associated with convergence along the western plate margin (F_{pcr}, plate contact resistance) and does not include the effects of topography. Subsequently, we investigate the effect of lateral variation in the magnitude of F_{pcr} and add the topography-related forces. The main results are: (1) A uniform magnitude of F_{pcr} leads to a better match with the observations than a magnitude that is a function of the dip of the lithosphere subducting below the western plate margin. (2) The amount of horizontal compression across the Andes, found in the case that ridge push is considered to be the only force driving the South American plate, is small compared to the value required to "sustain" the Andes.

Keywords: plate boundaries; orogeny; subduction zones; lithosphere

1. Introduction

In order to contribute to our understanding of the dynamics of the Andean Cordillera, the type locality of a non-collisional orogen, we investigate the forces that control the current state of stress in the mountain belt. From an observational point of view the present-day situation is the one best constrained and thus forms a natural point of departure for the investigations. The results obtained regarding the current situation may be used as a basis for subsequent work devoted to past stages and the temporal evolution of the forces. The Andes forms an excellent subject of study, in view of its relatively simple plate tectonic setting and given the large number of available observations.

We will not consider the mountain range as an isolated feature but study it as an integral part of the whole South American plate. Our study proceeds from a previous analysis in which we investigated the nature and magnitude of the forces that act on the

* Corresponding author. Tel.: +31 30 253 5091. Fax: +31 30 253 5030. E-mail: meijer@geof.ruu.nl

[1] Now at: Faculty of Earth Sciences, Utrecht University, The Netherlands.

PII S0012-821X(97)00029-0

South American plate applying the criterion that the plate, as a whole, must be in dynamic equilibrium [1]. This previous study provided us with a range of possible combinations of the plate tectonic forces. In the present study, a numerical model is used to compute intra-plate stress fields associated with several force distributions and the results are evaluated with observations of the actual stress field, such as are provided by earthquake focal mechanisms and geological analysis of fault kinematics.

Our approach is an improvement of previous work on the Andes in which the state of stress in the mountain range has been addressed only in terms of a vertical cross section (e.g., [2–4]). An approach similar to ours was followed recently by Coblentz and Richardson [5]. The work presented here is different, among other things, in that we will analyse in greater detail the observations and model results concerning the state of stress along the Andes.

Our study concentrates on two aspects: (1) The nature of the force associated with subduction below the western margin of the South American plate. (2) The relation between the regional stress field associated with the plate tectonic forces and the stresses that arise locally within the Andes as a result of topography and its compensating crustal/thermal root. On the basis of the dynamic analysis [1] we define a reference model that involves a uniform magnitude of the force associated with subduction below the western plate margin and excludes any effects of topography. Subsequently, lateral variation in resistance on the western margin and the forces due to topography are studied separately as modifications of the reference model. First, the available observations regarding the present-day stress field will be discussed.

2. Observed present-day stress field

Our main source of information regarding the current stress field is the World Stress Map data base (''WSM'', [6]), the South American part of which was compiled by Assumpção [7]. Earthquake focal mechanisms and geological field observations of recent and active faulting constitute the majority of the data (Fig. 1). In addition, there is information from borehole breakouts and volcanic alignments.

The WSM data have been supplemented with observations published in more recent years. Data quality was assigned according to WSM criteria. Additional earthquake focal mechanisms were taken from Assumpção and Araujo [9] for the Andes of Chile and northwest Argentina. The Harvard Centroid Moment Tensor (CMT) Catalogue ([10], now published with the US National Earthquake Information Center (NEIC) Preliminary Determination of Epicenters Catalog) was scanned for the period June 1990 through December 1992 (i.e., for the period after which CMT data are included in the WSM). Also, we included the result of an inversion of earthquake data for northwest Argentina [11]. Supplementary geological observations are reported by Dumont [12] for the Andean foreland of eastern Peru.

Focal mechanisms of earthquakes in the Andes south of 5°N mainly indicate reverse faulting consistent with WSW–ENE to E–W orientated compression (Fig. 1). Seismic intra-plate faulting is concentrated east of the high ranges. In particular, it occurs in the Sub-Andean foreland fold-and-thrust belt of Peru, Bolivia, and Argentina. Whereas reverse faulting dominates, strike-slip faulting is also observed. The existence of horizontal compression is confirmed by geological observations. The latter observations also show that normal faulting associated with roughly N–S orientated tensional stress characterises the high Andes at several places. Thus, ascending the Andes from the east, we find a change in tectonic regime from reverse faulting to normal faulting (e.g., [2]). As shown in Fig. 1c most reverse faulting occurs where the topography (averaged over an $1° \times 1°$ area centred on the epicentre or field site) is less than about 2 km. Normal faulting is observed at elevations exceeding 3 km. We may note that the two regimes are apparently not separated by an elevation interval where strike-slip faulting prevails. Data from the western flank are indicated with deviating symbols in Fig. 1. Close to the Pacific coast of south Peru normal faulting is observed to take place even at low elevations. There is only scant information about the tectonic regime as a function of depth in a given vertical column through the mountain range [13,14].

It has been noted previously that, on average, the direction of maximum horizontal compression

(σ_{Hmax}) expressed by observations from the Andes is close to both the direction of Nazca–South America convergence and the direction of absolute plate motion (e.g., [7]). When looked at in more detail, subtle trends in the orientation of σ_{Hmax} are discernable. Fig. 1b shows the available observations as a func-

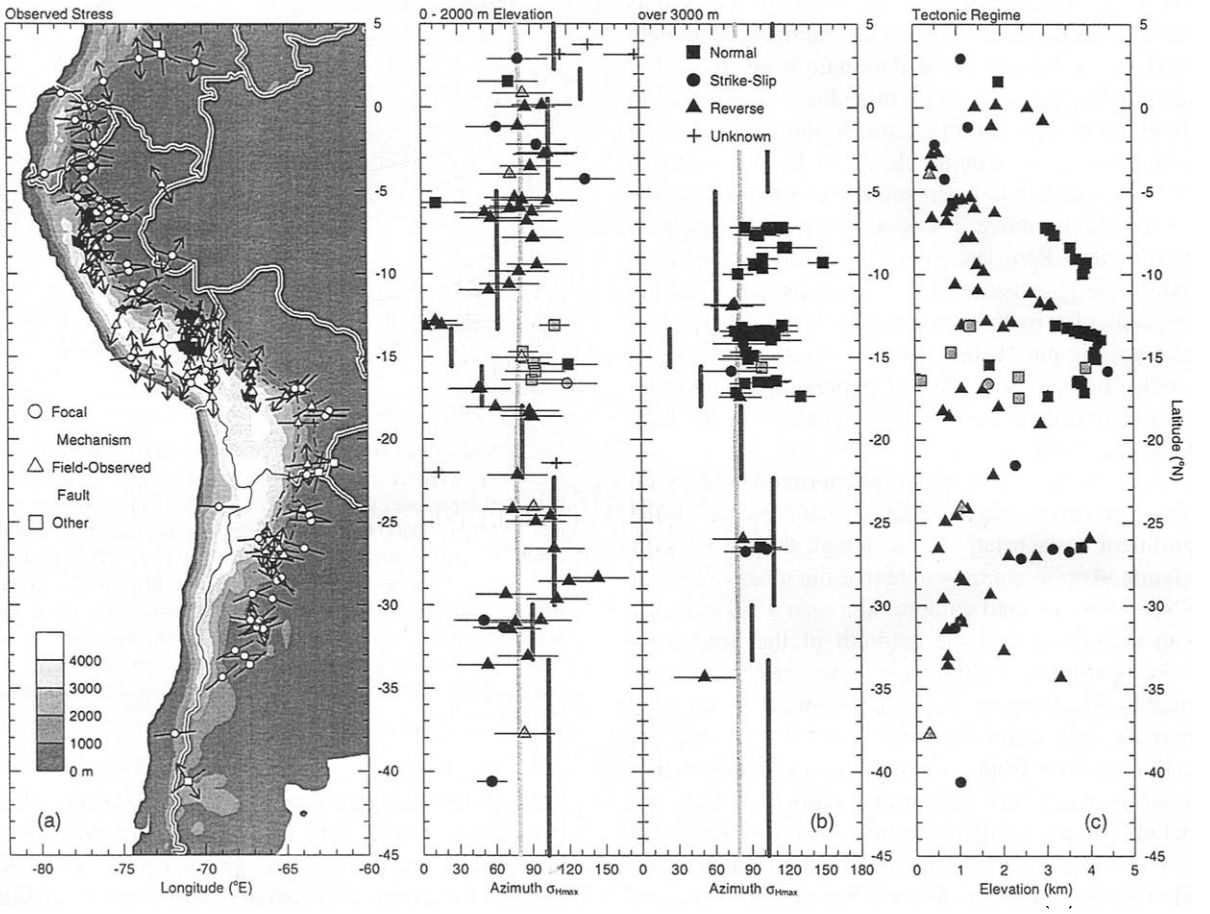

Fig. 1. Observations of the present-day state of stress in western South America. In all panels vertical axis gives latitude. (a) Map view of orientation of principal axes of stress shown against a background of contoured topography. For clarity, stress is shown for selected elements only. Short line = compression (σ_1) or P axis; double arrow = tension (σ_3) or T axis; symbols show type of stress indicator. Conventions regarding tectonic regime: σ_1 or P axis plunges less than 45° while σ_3/T axis plunges more than 45°: reverse faulting, only compressional axis is plotted; σ_1/P axis and σ_3/T axis both plunge less than 45°: strike-slip faulting, both axes are shown; σ_1/P axis plunges more than 45° while σ_3/T axis plunges less than 45°: normal faulting, only tensional axis is shown. Where the orientation of the axis of maximum horizontal compression is known but tectonic regime is not (borehole breakouts), only the compressional axis is plotted. Horizontal projections of the axes are show. Dash-dotted line delimits the Sub-Andean foreland fold-and-thust belt. Political borders indicated for reference. (b) Azimuth of the axis of maximum horizontal compression (σ_{Hmax}) as a function of latitude for two intervals of average topographic elevation (average elevation of the Earth's surface within a $1° \times 1°$ area centered on the epicentre or field site). For earthquake focal mechanisms and geological data σ_{Hmax} corresponds, respectively, to the horizontal projection of the P axis and σ_1 axis. Note: symbol type now indicates tectonic regime. Grey symbols pertain to the Andes west of the Altiplano–Puna plateau. Horizontal lines give uncertainty in azimuth of σ_{Hmax}, as indicated by World Stress Map quality measure. In this panel only observations within or immediately adjacent to the Andes are included. Also shown as a function of latitude are the azimuth of Nazca–South America convergence according to NUVEL-1 (continuous light grey line; [8]) and the orientation of a vector approximately perpendicular to the strike of the Andean Cordillera (dark grey, segmented line). Nazca–South America convergence has been evaluated at the trench. Both grey lines are the same for the two elevation intervals. (c) Tectonic regime as a function of latitude and average topographic elevation. Symbol type indicates tectonic regime as in (b).

tion of latitude and grouped according to average topographic elevation. For topography up to 2 km, going south from 3°N to 11°S, a, on average, more or less stable azimuth for σ_{Hmax} can be observed. North of this region several borehole break-outs indicate a markedly larger azimuth; immediately south of 11°S a cluster of data with a much smaller azimuth is observed. From this cluster southward to about 28°S data for the same topographic interval demonstrate an azimuth closer to E–W. South of 29°S the azimuth is again somewhat smaller. For the normal faults above 3 km we may infer that data from central Peru (including the Cordillera Blanca) show a σ_{Hmax} azimuth — taken as the direction perpendicular to the axes of tension — that is, on average, similar to that for the observations to the south. The last panel clearly expresses the non-uniform spatial distribution of observations in the high Andes.

Also shown in Fig. 1b is the approximate azimuth of the direction perpendicular to the strike of the cordillera at each latitude. Although the overall correlation is poor, we may note that the observations of NNE–SSW directed compression near 13°S coincide with a minimum in the azimuth of the normal-to-strike direction. Furthermore, the observations of roughly NE directed σ_{Hmax} between 30°S and 34°S more or less coincide with a segment where the Andes deviates from its general trend. A correlation between σ_{Hmax} orientation and normal-to-strike direction for the focal mechanisms around 30°S was previously pointed out by Assumpção and Araujo [9]. The normal faults above 3 km are characterised by σ_{Hmax} that significantly deviates from the normal-to-strike direction. In other words: tension is not directed parallel to the mountain range (cf. [7,14]). Moreover, the orientation of tension does not correlate with latitudinal changes in the strike of the mountain range [7].

3. Description of modelling procedure

3.1. Force modelling

As a basis for the present study we adopt the first-order model for the dynamics of the South American plate that was proposed previously on the basis of knowledge regarding the nature of the plate boundaries (Fig. 2; [1]). Incorporated are ridge push (F_{rp}), which drives the plate westwards and is counteracted by resistance associated with transform faults (F_{tf}), plate contact resistance due to subduction below the west margin (F_{pcr}), and resistance associated with Caribbean–South America convergence (F_{Car}). The ridge push force should be considered a horizontal pressure gradient, resulting from the cooling and contraction of oceanic lithosphere with age, integrated over the area of the oceanic part of the plate [16–18]. Plate contact resistance is modelled as a force parallel to the direction of convergence at the western plate margin which is, along most of the margin, the direction of Nazca–South America relative motion. South of 49°S the down-going lithosphere pertains to the Antarctic plate. F_{pcr} is assumed to act on the vertical western face of our plate model, which is a simplification of the actual situation in

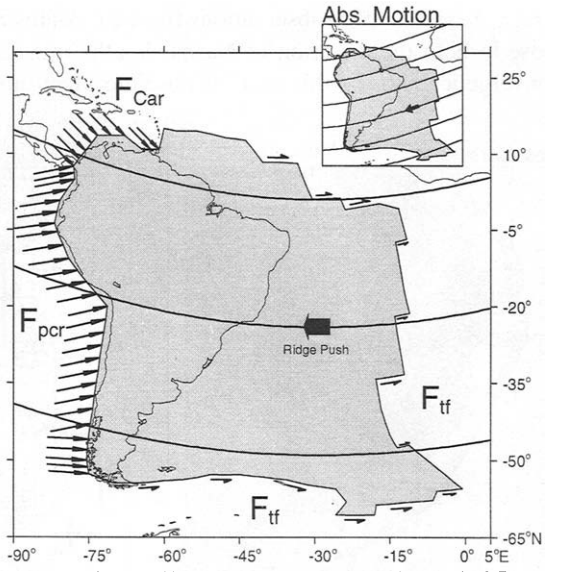

Fig. 2. Force distribution of the first-order model. Small circles are drawn with respect to the ridge push torque. Incorporated boundary forces are: F_{tf} = transform fault force; F_{pcr} = plate contact resistance; and F_{Car} = resistance due to Caribbean–South America convergence, shown here with azimuth N135°E. It is assumed no (net) forces are exerted on the plate in the Lesser Antilles and South Sandwich subduction zones or along the contact with the North American plate. Basal drag force is assumed to be (anti-)parallel to the direction of absolute plate motion. Inset shows absolute motion according to model HS2-NUVEL1 [15].

which the contact between the down-going and overriding plates dips eastwards. To first approximation, the magnitude of F_{pcr} is taken to be uniform along the margin. Regarding F_{Car}, a range of possible orientations was considered in [1]. Finally, we include basal drag force (F_{dr}) in the form of a shear stress σ_{dr} parallel to the direction of absolute plate motion, as predicted by model HS2-NUVEL1 [15], the most recent estimate available. We will consider both the possibility that basal shear acts as a resistive force and the possibility that basal shear constitutes a driving force. Ridge push and, when accounted for, forces associated with topography, can be quantified independently and enter the problem as known quantities. The magnitudes of F_{tf}, F_{pcr}, and F_{Car} are then determined as a function of σ_{dr} from the requirement that the net torque on the plate must vanish in order for the plate to be in equilibrium. Details concerning the method of computation can be found in [1]. Torque data pertinent to the present study are listed in Table 1. Minor differences with torques calculated previously [1] reflect the use of a mesh with smaller elements (see below). In contrast to [1] no F_{Car} is taken to act on the NW–SE striking segment of the Caribbean–South America boundary. This modification hardly affects the torque balance but was found to yield a more realistic stress field where the boundary strikes parallel to the applied force. Note that the "unscaled" torque magnitudes listed in the fifth column of Table 1 pose no constraint on the magnitudes these torques may attain in the experiments presented below.

3.2. Intra-plate stress calculations

Stress fields are obtained by modelling the South American plate as a thin elastic shell; calculations are performed with the Finite Element (FE) method. The plate's curved surface is approximated by a total of 3848 flat triangular elements of the linear displacement type. The distance between two E–W rows of nodal points and between subsequent nodes of a given row amounts to 150 km. These dimensions were chosen in order to be able to examine the stress field in the Andes and constitute a considerable reduction in element size in comparison with the mesh adopted in [1]. Stress fields are calculated assuming plane stress, Young's modulus is taken as 7×10^{10} N/m^2 and Poisson's ratio as 0.25. A reference thickness of 100 km has been adopted for the plate; no physical meaning should be attributed to this particular value. Stresses obtained with the FE model are horizontal, non-lithostatic stresses integrated over the plate's thickness. In subsequent fig-

Table 1
Torque data

Force	T_1 (10^{25} Nm)	T_2 (10^{25} Nm)	T_3 (10^{25} Nm)	Magnitude (10^{25} Nm)	Longitude (°E)	Latitude (°N)	Fig. 4	Fig. 5	Fig. 6	Fig. 7
rp	−3.799	2.068	−10.214	11.092	151.4	−67.0	1.000	1.000	1.000	1.000
tf	−2.101	1.676	−3.716	4.586	141.4	−54.1	−0.951	−1.163	−1.044	−1.764
Car	−0.665	−0.408	−0.816	1.129	−148.5	−46.3	−3.163	−2.624	−3.479	−2.767
dr	−0.065	1.131	−2.351	2.609	93.3	−64.3	0	0	0	5.000
pcr	0.296	1.722	−4.001	4.366	80.3	−66.4	−1.025	0	−1.134	−3.548
pcr-flat	0.142	0.434	−1.368	1.442	71.9	−71.6	0	−2.743	0	0
Andes	−0.373	0.215	−1.040	1.125	150.0	−67.5	0	0	1.000	1.000

Key to force type: rp = ridge push; tf = transform fault resistance; Car = force due to Caribbean–South America convergence; dr = basal drag; pcr = plate contact resistance; pcr-flat = plate contact resistance at flat segments only; Andes = net effect of Andean topography.
T_1, T_2, and T_3 are components of torque vectors in a Cartesian frame with x_1: 0°N, 0°E; x_2: 0°N, 90°E; x_3: 90°N. Ridge push and the effect of topography are quantified as described in the text. Torques of tf, Car, pcr, and pcr-flat are calculated for a force magnitude of 1×10^{12} Nm^{-1}. Listed basal drag torque corresponds to a basal shear stress of 0.1 MPa. Longitude and Latitude are coordinates of the torque pole. The last four columns give the factors by which the various torques must be multiplied in order to find the magnitude which they attain in the experiments in Fig. 4Fig. 5Fig. 6Fig. 7. Positive values of forces, basal shear stress, and multiplication factors denote a driving nature. Given the way the torques were derived, the scaling factors may be read as the magnitude of the corresponding force in units of 10^{12} Nm^{-1} (or 0.1 MPa for basal drag).

ures the stresses will be displayed as average values for a plate with the reference thickness of 100 km.

3.3. Incorporation of topography

Surface elevation has been derived from the ETOPO5 database (US National Geophysical Data Center), which provides topography on a $5' \times 5'$ grid. In order to account for the effect of topography we need to know how the topographic mass is compensated isostatically at depth. It has been suggested that the Altiplano–Puna plateau is compensated not only by a crustal root but also by a thermal root, due to a hot asthenosphere [19]. The relative importance of the two contributions is not known, however. In view of this uncertainty we will, as a first approximation of the actual situation, assume surface elevation to be compensated by a crustal root only, and assume constant (i.e., temperature independent) densities for crust and lithospheric mantle (respectively 2800 kg/m^3 and 3200 kg/m^3). Although the model thus incorporates a simplified density structure it will prove to offer important insight. We adopt a reference thickness for the continental crust of 35 km. Stresses or forces caused by topography are averaged over the plate thickness of 100 km. With the densities mentioned, the maximum tension resulting along the Andes amounts to about 57 MPa. Although our model offers insight into variations in stress between regions of different average surface elevation it does not allow us to evaluate the variation in stress *with depth below a given point*. In view of the nature of the available observations (see above) the latter does not pose a serious restriction.

The effect of topography is fully integrated in the finite element calculations. The method of calculation was outlined by Fleitout and Froidevaux [20] and Fleitout [21] and is in fact identical to the way ridge push is implemented [1]. Forces associated with topography or, in general, lateral changes in lithospheric structure, have recently been incorporated into intra-plate stress models for other regions also [22,23]. Some of the elements near the western plate margin encompass areas that are actually below sea level. The forces associated with these off-shore parts have been neglected so as not to "contaminate" the body forces corresponding to the Andes with effects related to the presence of the trench system.

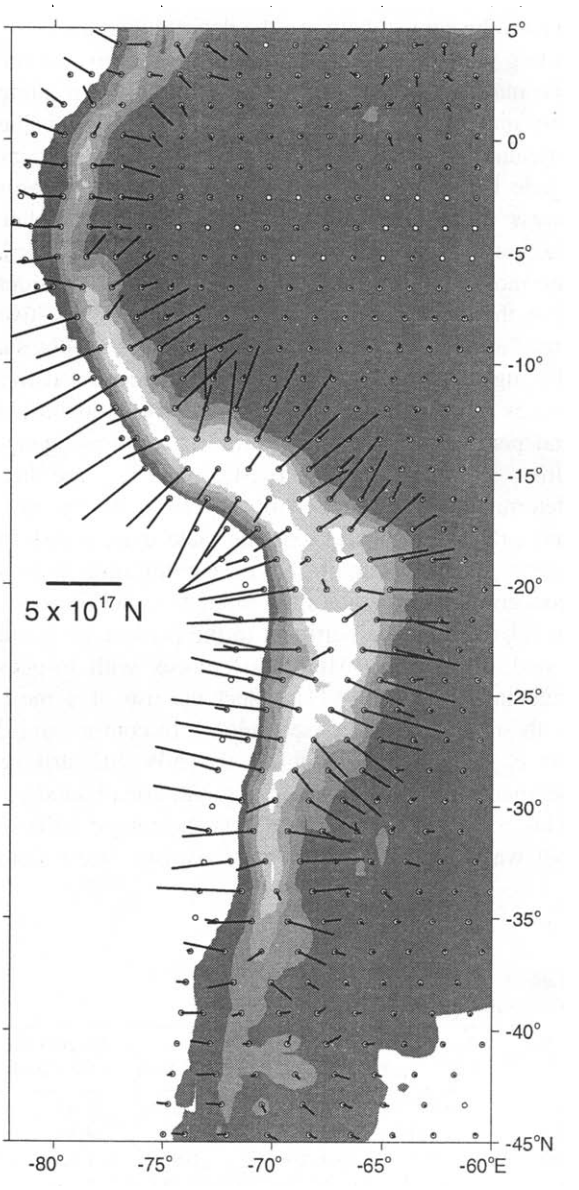

Fig. 3. Nodal point forces associated with the Andean Cordillera. Contoured topography as in Fig. 1a. White dots denote nodal points; black lines the associated forces.

The resulting nodal point forces are orientated in the down-slope direction (Fig. 3). The pole of the (small) net torque of the forces due to topography almost coincides with the pole of the ridge push torque (Table 1).

4. Analysis and results

4.1. Defining a reference model

As a starting point for the analysis we assume an azimuth for F_{Car} of N135°E and zero basal shear stress. This particular azimuth of F_{Car} is favoured on the basis of a comparison of stress fields calculated for several orientations of F_{Car} and the observations from, in particular, northwestern South America [24]. The assumption of zero basal shear stress implies that we take a neutral standpoint regarding the nature of basal shear stress (i.e., driving or resistive) and renders the model independent of assumptions regarding absolute plate motion. In the reference model a uniform magnitude of F_{pcr} is assumed and topography is not accounted for. The corresponding stress field (Fig. 4a) is characterised by E–W compression in the central part of the Andes. F_{Car} causes compression to rotate towards NW–SE in the northwestern part of the continent, including the northernmost Andes. The southern part of the Andes is characterised by a strike-slip regime with significant N–S tension in addition to the E–W compression. This

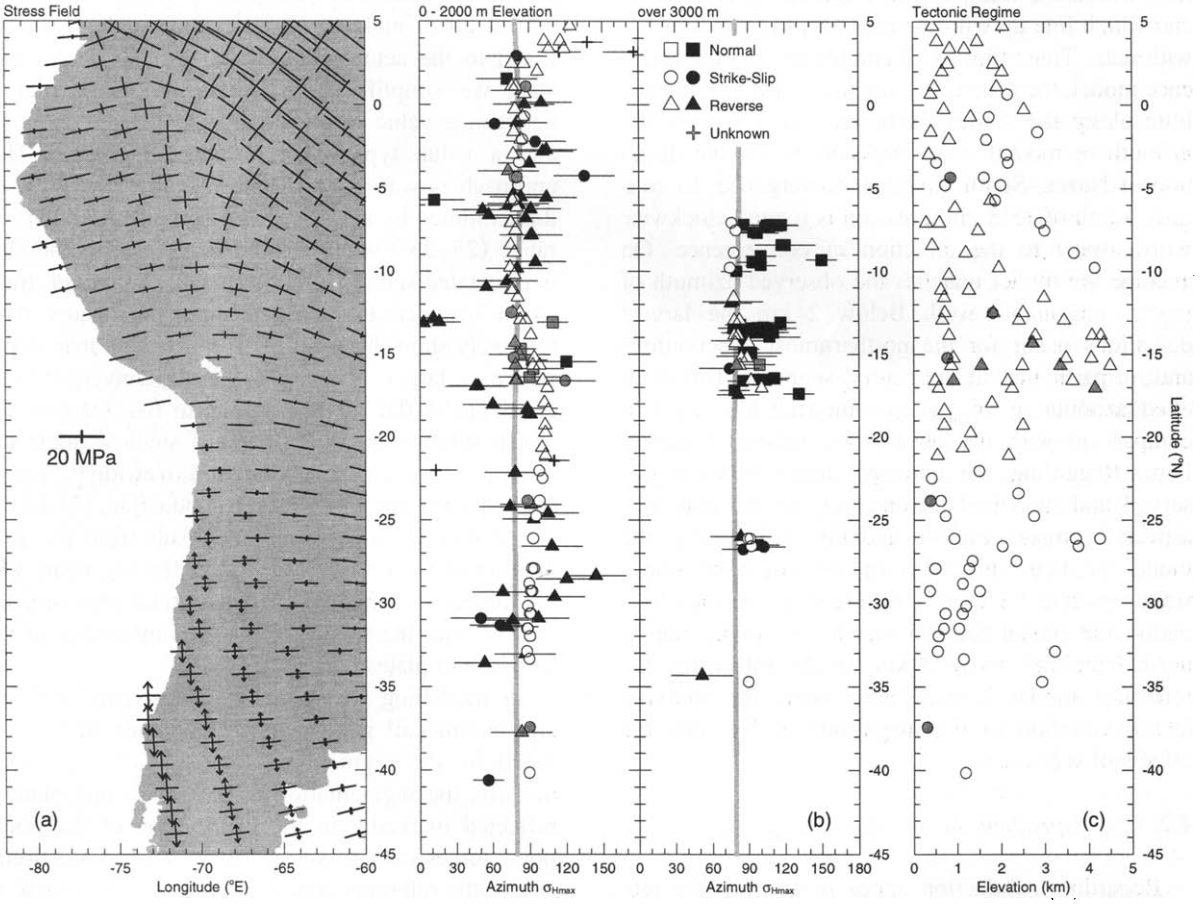

Fig. 4. (a) Intra-plate stress field calculated for the reference model. Short line = principal axis of compression; double arrow = principal axis of tension. Shown are horizontal non-lithostatic principal stresses averaged over the plate thickness of 100 km (at selected elements). Associated tectonic regime as follows, both horizontal axes compressive: reverse faulting; one axis compressive, the second tensile: strike-slip faulting; both axes tensile: normal faulting. (b) Latitudinal distribution of the modelled orientation of the principal axis of maximum horizontal compression as indicated by open symbols (or grey symbols without error bars) overlying a plot of observations identical to Fig. 1b. Symbol type for both model result and data indicates tectonic regime. (c) Modelled variation of tectonic regime as a function of latitude and topographic elevation (averaged over the corresponding elements). Compare Fig. 1c.

component of tension results from the east-directed shear on the southern plate boundary (Fig. 2).

Fig. 4b shows the model-derived azimuth of the principal axis of maximum compression and the tectonic regime for each element that encompasses a least one observation within its three sides. We adopted the grouping according to topographic elevation that was used to construct Fig. 1. Observations situated on the western flank of the Andes are denoted in lighter shade. For elevation below 2 km modelled stress is also depicted at latitudes where observations are absent. These extra points correspond to elements with an average topography which falls within the limits of the given elevation interval and which line up with the elements that do coincide with data. Thus, Fig. 4b illustrates that, in the reference model, the azimuth of calculated σ_{Hmax} changes little along the Andes. Between 3°N and 13°S the azimuth of modelled compression equals the direction of Nazca–South America convergence. In contrast, south of 13°S compression is rotated clockwise with respect to the direction of convergence. On average the model matches the observed azimuth of σ_{Hmax} reasonably well. Below 2 km the largest deviations occur for the northernmost observations and, in particular, at the central segment. The modelled azimuth of σ_{Hmax} is somewhat too small in comparison with the observations above 3 km in Peru. Regarding the correspondence between observed and modelled tectonic regime we note two aspects (compare Fig. 4c and Fig. 1c). Firstly, the model predicts strike-slip in the southern Andes where reverse faulting is observed to prevail. Secondly, the model fails to match the occurrence of normal faulting above 3 km. In the following, the reference model is used as a basis for studying lateral variation in the magnitude of F_{pcr} and the effects of topography.

4.2. F_{pcr} dependent on slab dip

Regarding subduction zones in general, the tectonic regime of the overriding margin has been found to correlate with the dip of the downgoing slab. Extensional "Marianas-type" overriding margins are mainly situated over steeply dipping plates, whereas compressional "Andean-type" margins tend to develop over slabs that dip more shallowly [18,25–27]. Likewise, lateral changes in the geology of the Andes have been attributed to a segmentation of the Nazca plate in the direction parallel to the trench (e.g., [28]). Generally speaking, the age of the descending lithosphere and the rate of convergence are considered to be the primary controls on slab dip [29]. In the case of subduction below the west margin of South America, only slab age can contribute to the segmentation: the rate of convergence of the Nazca plate and South America changes little along their contact [30,31]. Only in the southernmost Chile trench, where the approaching oceanic lithosphere is part of the Antarctic plate, does convergence occur at a deviating, much slower, rate.

Instead of making the magnitude of F_{pcr} proportional to the actual angle of dip of the descending slab, we simplify the situation by differentiating between a value characteristic for "flat" segments and a value typical for "steep" segments. This approach is warranted by the fact that the angle of dip exhibited by the steep segments falls in a narrow range (25–35°) while at both flat segments the slab is orientated subhorizontally [11,32]. Moreover, transition between the various segments occurs over relatively short distances. The upper plate may experience a larger resistance due to convergence at segments of flat subduction due to two reasons: (1) When subduction occurs under a shallow angle the interface between downgoing and overriding plate is larger than in the case of steep subduction. (2) To the extent that shallow dip angles result from the subduction of young lithosphere, the flat segments will be subject to a relatively high normal pressure, resulting from the small gravitational instability of the downgoing plate.

In modelling we consider the extreme situation and assume all plate contact resistance to be provided by the segments of flat subduction. Consequently, the segmentation of the subducting plate is reflected markedly in the distribution of the nodal point forces on the western margin (Fig. 5a). Relative to the reference model the maximum increase in compression inwards from the flat segments is by a factor of about 2.7 (Fig. 5b, see also Table 1). Compression fans out from the segments of shallow subduction. N–S tension in southern Chile is much amplified. Tension roughly parallel to the western margin is also developed in the central Andes.

The effect of the lateral variation in F_{pcr} on the orientation of compression is illustrated by Fig. 5c. In general, the present model predicts orientations of maximum horizontal compression that deviate more from the observed orientations than does the reference model. In other words, implementation of a dependence on slab dip causes the model curve in Fig. 5c to move away from the data. Although the deviation is largest in the present model, the same tendency will also characterise models with less extreme differences between flat and steep segments.

4.3. Incorporation of topography

Reference model as Background: When the forces associated with the thickened crust (Fig. 3) are incorporated we obtain the stress field shown in Fig. 6a. Much of the Andes is now characterised by tensional stress; tension is largest in the direction roughly normal to the strike of the range. Topography also affects the state of stress in the foreland east of the Bolivian orocline. The effect of topography on the orientation of σ_{Hmax} is clearly expressed in Fig. 6b. For observations below 2 km the model poorly matches the observed azimuth of σ_{Hmax} north of 12°S. In contrast, further south, the fit is improved compared to the previous case: the model matches well the latitudinal changes in σ_{Hmax} azimuth. Above 3 km the large cluster of observed normal faults near 15°S is matched well but significant differences are found with the observations in the Cordillera Blanca region and the data from northwest Argentina. With

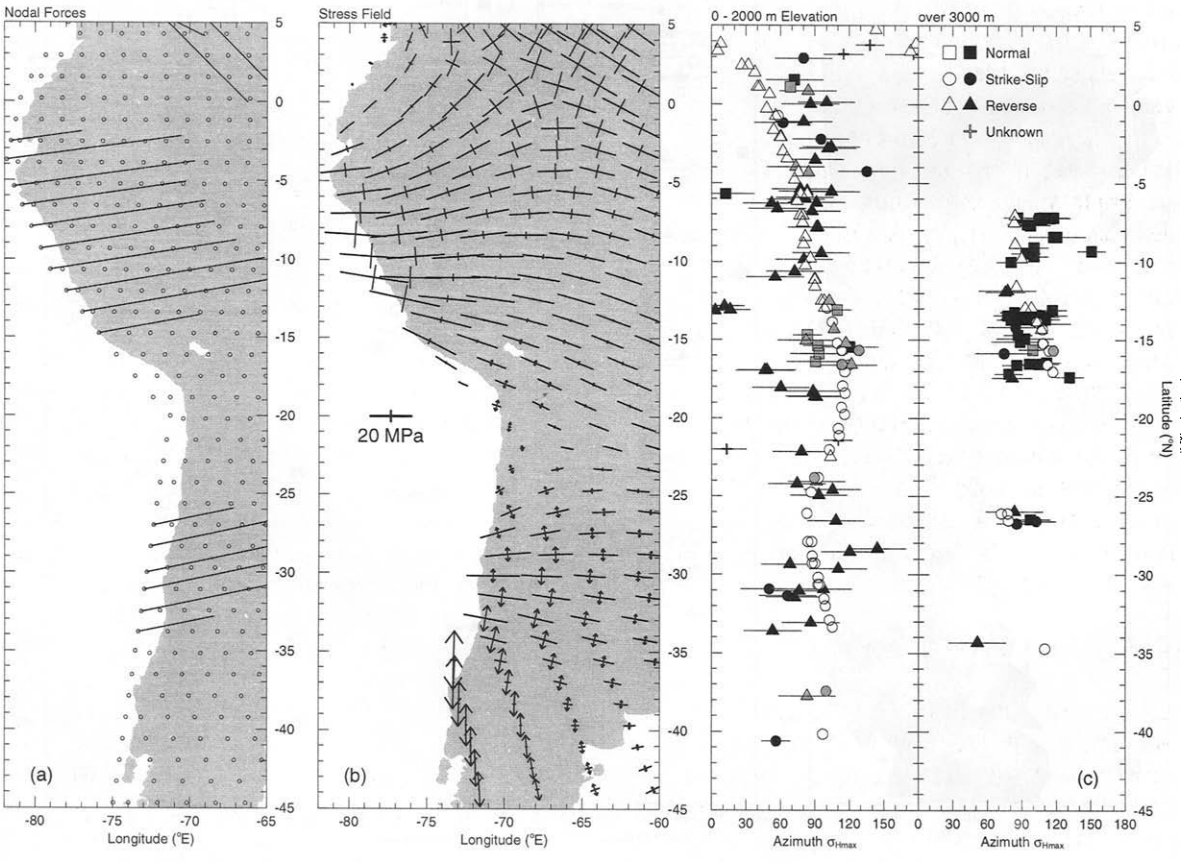

Fig. 5. (a) Nodal point forces of the model with dip-dependent F_{pcr}. (b) and (c) Associated stress field and latitudinal distribution of the azimuth of maximum compression in the manner of Fig. 4a,b.

respect to the tectonic regime we find that the model is in disagreement with the observations. Even at low elevations normal faulting is predicted, whereas in reality reverse faulting prevails (compare Fig. 6c and Fig. 1c).

Background model with driving basal shear: The last result has two possible explanations: either we are overestimating the effect of topography, or we underestimate the amount of compression due to plate tectonic forces (i.e., the amount of compression present in the reference model). Variation within reasonable limits of the densities used to represent the Andes was found not to reduce the effect of topography significantly. Thus, let us for the moment assume that the cause for the inferred failure of the models resides entirely on the side of the reference model. For the magnitude of intra-plate compression near the western margin to be larger it would require a more resistive F_{pcr}. Generally speaking, the latter would require an extra driving force to be acting on the South American plate. Within the framework of our first-order model such an extra driving force can only be provided by shear at the base of the lithosphere.

Fig. 7a shows the stress field we obtain when a uniform driving basal shear stress of 0.5 MPa is incorporated. The presence of a larger "background" compression is expressed in the orientation of the axis of maximum tension: the latter has rotated away from the normal-to-strike direction, towards an orien-

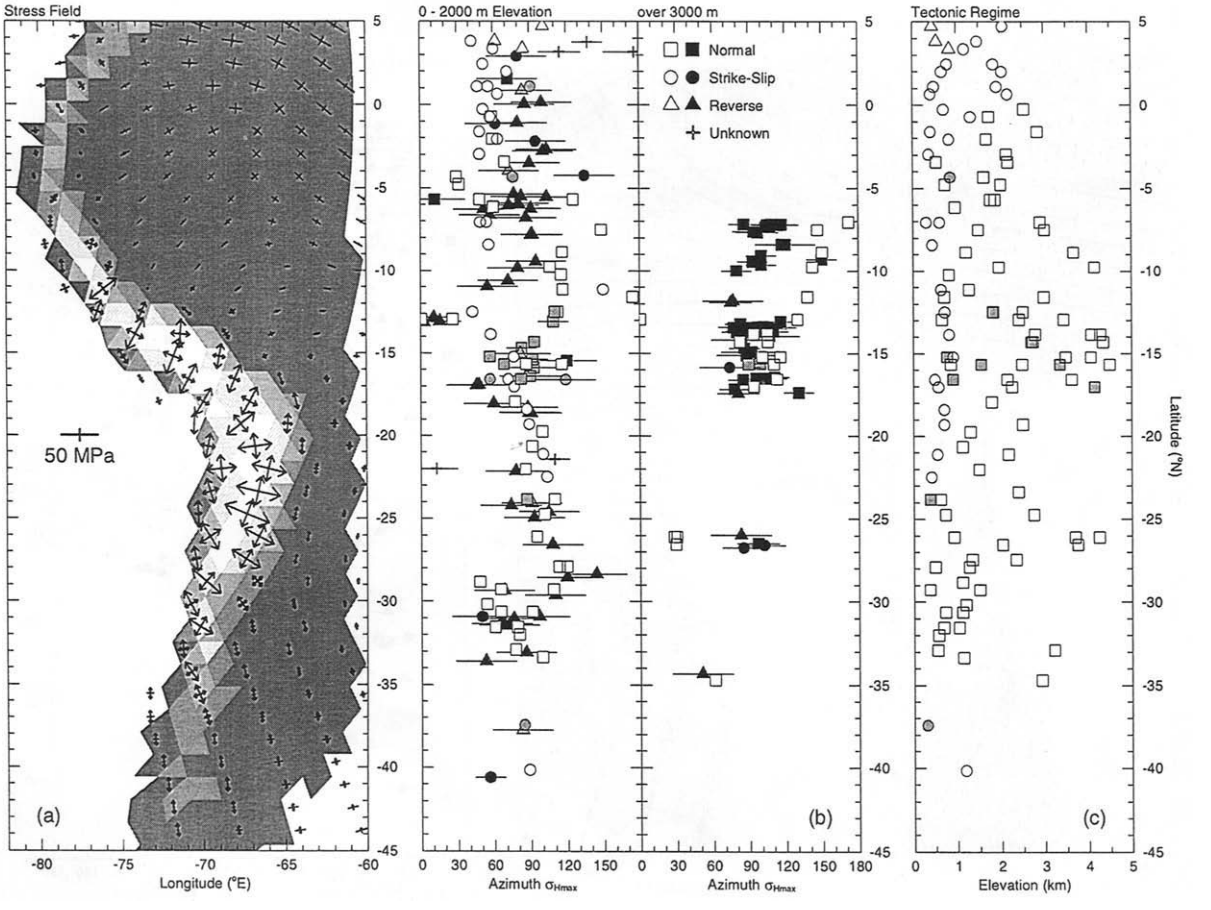

Fig. 6. Model results in case the forces associated with topography (Fig. 3) added to the reference model. Arrangement of panels as in Fig. 4.

tation more perpendicular to the background compression (see also Fig. 7b). For elevations below 2 km, the changes observed in the azimuth of σ_{Hmax} south of 12°S are matched to a lesser degree by the present model than by the corresponding model with σ_{dr} equal to zero (Fig. 6b). North of 12°S the model does better than before for elevations below 2 km. Above 3 km the normal faults of the Cordillera Blanca and northwest Argentina are also reasonably matched. With respect to the model-derived tectonic regime, Fig. 7c illustrates that elevations below 3 km are characterised mostly by strike-slip and that normal faults occur in particular above 3 km. Above 3 km, at some latitudes, the model predicts strike-slip where normal faults are observed. However, the magnitude of any additional E–W compression is always very small.

5. Discussion

5.1. Dip-dependence of F_{pcr}

It is clear from the results presented in the above that none of our models is ''preferred'' in the sense that it provides a match to all aspects of the actual stress field. Between them, however, the model experiments offer important insights. First of all, under the assumption that the intra-plate stress field is mainly controlled by F_{pcr}, it would appear that the available observations rule out the possibility of a

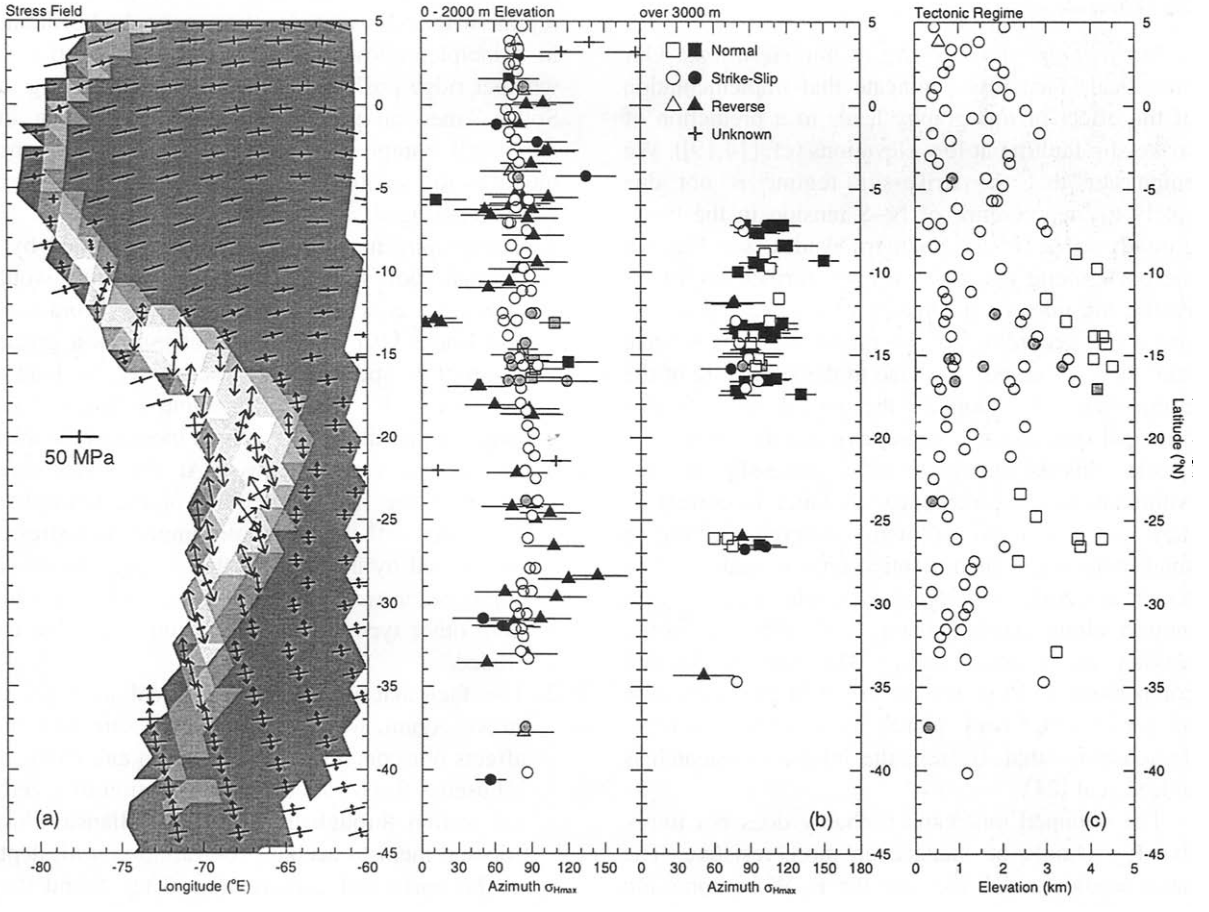

Fig. 7. Results obtained for the experiment in which the forces associated with topography are incorporated and a driving basal shear stress of 0.5 MPa is assumed. Arrangement of panels as in Fig. 4.

relation between F_{pcr} and slab dip. This conclusion was found to be unaffected when, in addition to a dip-dependent F_{pcr}, the role of topography was accounted for or when a driving basal shear stress was introduced.

Our conclusion is remarkable in view of the fact that other aspects of the Andean orogen, such as topography and style of deformation, do seem to correlate with the dip of the downgoing plate [28,33,34]. For example, it was pointed out by Gephart [34] that the along-strike extent of the Altiplano–Puna approximately coincides with the central segment of relatively steep subduction. Perhaps, rather than controlling the amount of compressive stress transmitted to the margin of the overriding plate, the angle of subduction affects the response of the margin to such stresses.

5.2. The role of topography

Implications of strike-slip at low elevations: Our numerical calculations indicate that implementation of the effect of topography leads to a prediction of strike-slip faulting at low elevations (cf. [14,19]). We emphasize that the strike-slip regime is not due solely to the presence of N–S tension in the background model (in the southern Andes, see Fig. 4): the background tension is always further amplified. Partly, the inferred mismatch in tectonic regime — strike-slip according to the model whereas reverse faulting is observed — is due to the simplicity of the comparison. As soon as the model predicts one principal stress to be compressive and the other to be tensile, this is classified as a strike-slip regime. Although, strictly speaking, the latter is correct, it may distort comparison with observed faulting: a small component of horizontal tension additional to major horizontal compression could well lead to motion along a pre-existing fault that we would classify as reverse faulting. However, a detailed comparison — in which the effect of the orientation of pre-existing fault planes is accounted for — demonstrates that, overall, the inferred mismatch is indeed real [24].

The obtained mismatch probably does not imply that F_{pcr} should be made even more resistive. The latter would further increase the E–W compression but would not prevent the second horizontal principal stress, which is almost zero in the background model, from becoming tensile due to topography. Moreover, a further increase in E–W compression would lead to an increasing misfit to the normal faulting observed at high elevations.

A possible implication of the mismatch obtained is that the background stress field is not correct. When, in reality, the regional stress field features compression in both horizontal directions, reverse faulting would extend to higher elevations. Alternatively, the discrepancy between model and reality may indicate that deformation in the Andes cannot be fully represented by means of a homogeneous and isotropic elastic model; our experiments would thus offer valuable insight into the mechanical behaviour of the mountain range.

Does ridge push constitute the only driving force? The constraint on the magnitude of horizontal compression offered by the observed change in tectonic regime with increasing elevation in the Andes should, in principle, allow us to answer the question of whether ridge push forms the only force driving the South American plate. We have inferred that the horizontal compression predicted by our reference model is too small. Three potential sources of error can be envisaged:

1. Topography may, in part, be compensated by a thermal root. It is not obvious how this would affect our conclusions. As stated by Froidevaux and Isacks [19], a thermal root implies a greater depth of compensation. Consequently, the load of topography is "felt" throughout a larger depth range of the lithosphere, which increases the average excess vertical stress. At the same time, however, the rise in the base of the lithosphere associated with a thermal root implies that stresses are carried by a thinner plate: average horizontal compression would also be increased [4]. In addition, other types of compensation cannot be excluded.
2. The fact that we consider vertical averages of stress. Again, we do not know for sure how this affects our conclusions. Richardson and Coblentz [4] used a finite element representation of a vertical section through the Cordillera Blanca which allowed them to account for variation with depth in the horizontal compression. They found that, relative to the situation with a uniform depth distribution, a larger amount of total horizontal

compression would still provide a match with the observations. In this case, our conclusion that the reference model provides too little horizontal compression would be further strengthened.

3. The fact that the model predicts strike-slip where reverse faulting is observed. Although the implications of this are uncertain, it does not necessarily imply that conclusions regarding the required amount of horizontal compression are wrong.

Relevant to the latter question is the relative magnitude of the vertical principal stress and the horizontal *across-strike* principal stress. Thus, in conclusion, we state that the model calculations certainly suggest that horizontal compression in the reference model is too small to explain the observed state of stress in the Andes but that the experiments also illustrate the considerable uncertainty involved.

As mentioned in the introduction, another analysis of the South American intra-plate stress field was recently carried out by Coblentz and Richardson [5]. There are three notable differences between the latter study and that reported here: (1) different types of forces are incorporated; (2) in [5] all forces except basal drag are assigned a magnitude at the outset and both the orientation and magnitude of basal drag are solved for; (3) in [5] the predicted magnitudes of the principal stresses and the tectonic regime are studied in an E–W section through the entire plate that includes the Andes of central Peru. We have examined the stress field (including the orientation of the principal axes) in detail along the length of the Andes. These differences in approach preclude a straightforward comparison of the two investigations. However, although the absolute values of the various forces involved are different, our study and that of Coblentz and Richardson [5] agree on the fact that an additional driving force appears to be required.

Finally, we emphasize that this additional driving force need not necessarily be a *uniform* basal shear stress. It is possible that any driving basal shear is largest below the continental part of the South American plate or is located near the spreading ridge.

6. Conclusions

The Andean Cordillera provides a unique possibility for studying the state of stress (in particular, the occurrence of normal faults at high altitude) in an orogenic belt at an active continental margin. We used a thin elastic shell model of the entire South American plate, in which the Andes are embedded, to investigate the forces that are expected to be the primary controls on the state of stress in the mountain range.

The following conclusions were reached:

1. A uniform distribution of the resistance on the western margin provides a better overall fit to the available observations than a dip-dependent distribution of magnitude.
2. In order to match the observation that normal faulting in the Andes is restricted to elevations exceeding 3 km, we need to invoke an amount of horizontal compression that is large compared to the value found where ridge push is the only driving force. The results thus suggest that an extra driving force, additional to age-dependent ridge push in the manner implemented in our study, may be acting on the South American plate.

Acknowledgements

The authors would like to thank M. Assumpção for his clarification of aspects of the stress data and R.M. Richardson for providing a highly constructive review. We also thank a second, anonymous, reviewer. MJRW received support from NWO-Pionier Project PGS 76-144 "Detailed Structure and Dynamics of the Upper Mantle". This is Geodynamics Research Institute (Utrecht University) contribution 97.001. ***[PT]***

References

[1] P.Th. Meijer, M.J.R. Wortel, The dynamics of motion of the South American plate, J. Geophys. Res. 97 (1992) 11915–11932.

[2] B. Dalmayrac, P. Molnar, Parallel thrust and normal faulting in Peru and constraints on the state of stress, Earth Planet. Sci. Lett. 55 (1981) 473–481.

[3] C. Froidevaux, S. Uyeda, M. Uyeshima, Island arc tectonics, Tectonophysics 148 (1988) 1–9.

[4] R.M. Richardson, D.D. Coblentz, Stress modelling in the Andes: constraints on the South American intraplate stress magnitudes, J. Geophys. Res. 99 (1994) 22015–22025.

[5] D.D. Coblentz, R.M. Richardson, Analysis of the South American intraplate stress field, J. Geophys. Res. 101 (1996) 8643–8657.
[6] M.L. Zoback, First- and second-order patterns of stress in the lithosphere: the World Stress Map Project, J. Geophys. Res. 97 (1992) 11703–11728.
[7] M. Assumpção, The regional intraplate stress field in South America, J. Geophys. Res. 97 (1992) 11889–11903.
[8] C. DeMets, R.G. Gordon, D.F. Argus, S. Stein, Current plate motions,, Geophys. J. Int. 101 (1990) 425–478.
[9] M. Assumpção, M. Araujo, Effect of the Altiplano–Puna plateau, South America, on the regional intraplate stresses, Tectonophysics 221 (1993) 475–496.
[10] A.M. Dziewonski, J.H. Woodhouse, An experiment in systematic study of global seismicity: Centroid-moment tensor solutions for 201 moderate to large earthquakes of 1981, J. Geophys. Res. 88 (1983) 3247–3271.
[11] T. Cahill, B.L. Isacks, D. Whitman, J.-L. Chatelain, A. Perez, J.M. Chiu, Seismicity and tectonics in Jujuy province, Northwestern Argentina, Tectonics 11 (1992) 944–959.
[12] J.F. Dumont, Lake patterns as related to neotectonics in subsiding basins: the example of the Ucamara depression, Peru, Tectonophysics 222 (1993) 69–78.
[13] R.W. Allmendinger, M. Strecker, J.E. Eremchuk, P. Francis, Neotectonic deformation of the southern Puna plateau, northwestern Argentina, J. South Am. Earth Sci. 2 (1989) 111–130.
[14] J.L. Mercier, M. Sebrier, A. Lavenu, J. Cabrera, O. Bellier, J.-F. Dumont, J. Machare, Changes in the tectonic regime above a subduction zone of Andean type: the Andes of Peru and Bolivia during the Pliocene–Pleistocene, J. Geophys. Res. 97 (1992) 11945–11982.
[15] A.E. Gripp, R.G. Gordon, Current plate velocities relative to the hotspots incorporating the NUVEL-1 global plate motion model, Geophys. Res. Lett. 17 (1990) 1109–1112.
[16] C.R.B. Lister, Gravitational drive on oceanic plates caused by thermal contraction, Nature 257 (1975) 663–665.
[17] F.M. Richter, D.P. McKenzie, Simple plate models of mantle convection, J. Geophys. 44 (1978) 441–471.
[18] P. England, R. Wortel, Some consequences of the subduction of young slabs, Earth Planet. Sci. Lett. 47 (1980) 403–415.
[19] C. Froidevaux, B.L. Isacks, The mechanical state of the lithosphere in the Altiplano–Puna segment of the Andes, Earth Planet. Sci. Lett. 71 (1984) 305–314.
[20] L. Fleitout, C. Froidevaux, Tectonic stresses in the lithosphere, Tectonics 2 (1983) 315–324.
[21] L. Fleitout, The sources of lithospheric tectonic stresses, in: R.B. Whitmarsh, M.H.P. Bott, J.D. Fairhead, N.J. Kusznir, (Eds.) Tectonic Stress in the Lithosphere, R. Soc. London, London, 1991, pp. 73–81.
[22] R.M. Richardson, L.M. Reding, North American plate dynamics, J. Geophys. Res. 96 (1991) 12201–12224.
[23] D.D. Coblentz, M. Sandiford, Tectonic stresses in the African plate: constraints on the ambient lithospheric stress state, Geology 22 (1994) 831–834.
[24] P.Th. Meijer, Dynamics of active continental margins: the Andes and the Aegean Region, Geol. Ultraiectina 130 (1995) 1–224.
[25] F. Megard, H. Philip, Plio-Quaternary tectono-magmatic zonation and plate tectonics in the Central Andes, Earth Planet. Sci. Lett. 33 (1976) 231–239.
[26] P. Molnar, T. Atwater, Interarc spreading and Cordilleran tectonics as alternates related to the age of subducted oceanic lithosphere, Earth Planet. Sci. Lett. 41 (1978) 330–340.
[27] S. Uyeda, H. Kanamori, Back-arc opening and the mode of subduction, J. Geophys. Res. 84 (1979) 1049–1061.
[28] T.E. Jordan, B.I. Isacks, R.W. Allmendinger, J.A. Brewer, V.A. Ramos, C.J. Ando, Andean tectonics related to geometry of subducted Nazca plate, GSA Bull. 94 (1983) 341–361.
[29] M.J.R. Wortel, N.J. Vlaar, Age-dependent subduction of oceanic lithosphere beneath western South America, Phys. Earth Planet. Inter. 17 (1978) 201–208.
[30] M.J.R. Wortel, Spatial and temporal variations in the Andean subduction zone, J. Geol. Soc. London 141 (1984) 783–791.
[31] M.J.R. Wortel, S.A.P.L. Cloetingh, Accretion and lateral variations in tectonic structure along the Peru–Chile Trench, Tectonophysics 112 (1985) 443–462.
[32] W.D. Pennington, Subduction of the eastern Panama basin and seismotectonics of northwestern South America, J. Geophys. Res. 86 (1981) 10753–10770.
[33] B.L. Isacks, Uplift of the central Andean Plateau and bending of the Bolivian Orocline, J. Geophys. Res. 93 (1988) 3211–3231.
[34] J.W. Gephart, Topography and subduction geometry in the central Andes: clues to the mechanics of a noncollisional orogen, J. Geophys. Res. 99 (1994) 12279–12288.